MEASUREMENT OF THICKNESS OF THE GREENLAND ICE SHEET AND HIGH-RESOLUTION MAPPING OF INTERNAL LAYERS

David Braaten, Pannirselvam Kanagaratnam, Torry Akins, and Sivaprasad Gogineni

Radar Systems and Remote Sensing Laboratory
University of Kansas Center for Research, Inc.
2335 Irving Hill Road, Lawrence, Kansas 66045-7612, USA
785/864-4835 * Fax 785/864-7789 * kmason@ittc.ku.edu

RSL Technical Report 20780-2

March 2003

Sponsored by:

National Aeronautics and Space Administration Headquarters
Washington DC 20546

Grant No. NAG5-8758

1. Introduction

This is a final report on the project for the period between August 1999 and December 2002, with primary research goals of continuing ice thickness and bottom topography mapping using an airborne radar, and to develop remote sensing techniques for estimating snow accumulation rate with a high-resolution radar over glacial ice. During this period we have upgraded the radar depth sounder incrementally to improve its performance for collecting data on outlet glaciers and around the 2000-m contour line in southern Greenland. This project period included two Greenland field seasons (2001 and 2002).

As a part of NASA's Program for Arctic Climate Assessment (PARCA) initiative, we have been involved in ice thickness measurements over the Greenland ice sheet since 1993. Using low-power 150-MHz coherent radars, we have collected a large, consistent, geolocated data set of ice thickness for different regions of the ice sheet. We obtained good ice thickness information for over 90% of the flight lines flown over the Greenland ice sheet as a part of the PARCA initiative [Gogineni et al., 2001]. We have placed radar echograms and derived ice thickness data from these flights on a server at the University of Kansas (http://tornado.rsl.ukans.edu/Greenlanddata.htm) for easy access by the scientific community, and NSIDC maintains a link to these data.

We have issued periodic reports on the data collection and processing [Legarsky (1999), Tee et al. (1999), and Gogineni, Allen and Stiles(2000)], reported significant results in open literature [Kanagaratnam et al. (2001), Gogineni et al. (2001), Legarsky, Gogineni and Akins (2001), Braaten et al. (2002)] and have reported results in conference proceedings [Kanagaratnam et al. (1999, 2000, 2002), Legarsky et al. (1999), Gogineni and Kanagaratnam (1999), Gogineni and Kanagaratnam (2000), Leuschen, Gogineni, and Tammana (2000), Kanagaratnam, Eakin, and Gogineni (2001), and Braaten and Gogineni (2002)]. Instead of replicating here the results recorded in these reports, papers and conference proceedings, we will provide a summary of our significant accomplishments.

2. Significant accomplishments

Among the technical and research accomplishments achieved during this project were substantial improvements to the radar depth sounder, development of a high-resolution wideband radar, development of a calibrator for the wideband radar, standardizing signal processing procedures, and characterization of ice thickness and bed topography in outlet glacier regions.

2.1 Improvements to radar depth sounder

We improved radar depth sounder performance to collect data over outlet glaciers. Over outlet glaciers, ice-bed echoes are masked by the off-vertical surface clutter and multiple echoes between the aircraft and the ice surface. These modifications include:

1. Accurately measuring the system transfer function of the installed radar system to permit use of methods such as predictive deconvolution to eliminate or reduce multiple returns off the ice surface. The transfer function is also used to develop model-based signal processing algorithms to reduce off-angle clutter signals. This has been accomplished by developing a multiple range optical delay line and incorporating it into the system for measuring the system transfer function periodically during a flight. Now we are applying

this technique to data collected from Svalbard to remove multiple echoes that are masking the return from the ice-bed interface.

2. Modifying the system to transmit a simple 50 ns pulse without a chirp for data collection over several outlet glaciers in the south. The KU radar depth sounder transmits a 1.6-μs chirped pulse and uses 12-bit A/D converters to digitize received signals. The typical dynamic range of a 12-bit A/D converter is about 72 dB, whereas the dynamic range of received signals from ice is more than 120 dB. For most ice sheet measurements we use a Sensitivity Time Control (STC) to compress the signal dynamic range to match that of the digitizer. This is accomplished by reducing the receiver gain in the time window during which the primary and multiple echoes of the surface are received with a consequent reduction in receiver sensitivity. However, this reduction makes it difficult to observe weak echoes from outlet glaciers containing warm ice. Therefore, by transmitting an unchirped pulse and range gating the multiple echoes between the aircraft and the ice surface, we can obtain high sensitivity in outlet glacier areas. We need to gate out only one or two cells –10 m – with the unchirped pulse, whereas we would need to gate out about 150 m with a chirped pulse, which would also gate out ice-bed echoes. We will use this mode for collecting data during future missions over outlet glaciers with ice thickness of less than about 1000 m.

2.2 Development of a high-resolution wideband radar

Accurate determination of the spatial and temporal aspects of snow accumulation is essential to assessing the mass balance of the polar ice sheets. Traditionally, accumulation information is obtained from sparsely-distributed cores and pits. Surface-based high-resolution radars have been used to map near-surface internal layers for determining the variability of snow accumulation. However, coverage that can be obtained with a surface-based radar is limited, and a key goal in this project was the development of an airborne system. We designed and built an operational airborne wideband radar, which operates over the frequency range from 600 to 900 MHz for high-resolution mapping of the internal layers. It operates in FM-CW mode with a transmit power of 100 mW and uses TEM-horn antennas mounted in the bomb bay of a NASA P-3B aircraft. We have also developed a digital data acquisition system to collect and process data.

Figure 1 shows the block diagram of the operational wideband FM-CW radar. The heart of the radar is a Direct Digital Synthesizer (DDS) that can generate a chirp signal with a maximum frequency of 400 MHz using a 1-GHz clock signal. The clock signal is generated with a PLL oscillator. The PLL output is also used to generate all other signals needed to operate the radar, thereby making the system fully coherent. The Direct Digital Synthesizer (DDS) generates a chirped signal over the frequency range from 100 to 400 MHz. This signal is passed through a bandpass filter to eliminate spurious signals. Using an upconverter driven by a 500-MHz local oscillator signal derived from a 1-GHz PLL oscillator, the filtered chirp signal is upconverted into the 600-900 MHz frequency range. The upconverter output is filtered and leveled with a limiting amplifier to minimize amplitude variations across the chirp bandwidth. It is then passed through a directional coupler, a buffered power amplifier, a bandpass filter, and an attenuator to the antenna. The directional coupler is used to derive a sample of the transmitter signal to serve as the local oscillator for a mixer in the receiver.

The receiving antenna collects the reflected signal from the target and supplies it to the receiver. The RF section of the receiver consists of a bandpass filter, a buffered low-noise

amplifier, and a mixer. The bandpass filter is used to eliminate any spurious out-of-band signals from entering and saturating the receiver. The buffered low-noise amplifier is used to increase received signal level and provide reverse isolation. This amplifier is selected with very high reverse isolation to minimize local oscillator signal radiation by the receive antenna. In the mixer, the received signal is combined with a sample of the transmitter signal to generate beat frequency signals. In an FM-CW radar, the frequency of the beat-frequency signal is directly proportional to range. Thus, by spectrum analyzing beat-frequency signals, we can separate received signals from various layers or ranges.

The IF section of the receiver consists of a high-pass filter, two buffered amplifiers, a bandpass filter and a low-pass filter. A Gaussian-response high-pass filter with very little ringing is used to reduce directly coupled signals between the antennas from saturating the IF amplifiers. The two amplifiers are used to increase the received signal level to that required for proper digitization. The bandpass filter is used to eliminate higher order intermodulation signals generated in the mixer. The low-pass filter serves as an anti aliasing filter for digitization. A digital signal processor consisting of a 12-bit A/D converter and integrator is used to coherently average digitized signals to improve signal-to-noise ratio. These signals are stored and processed with an FFT algorithm to generate range profiles as a function of position along the flight path.

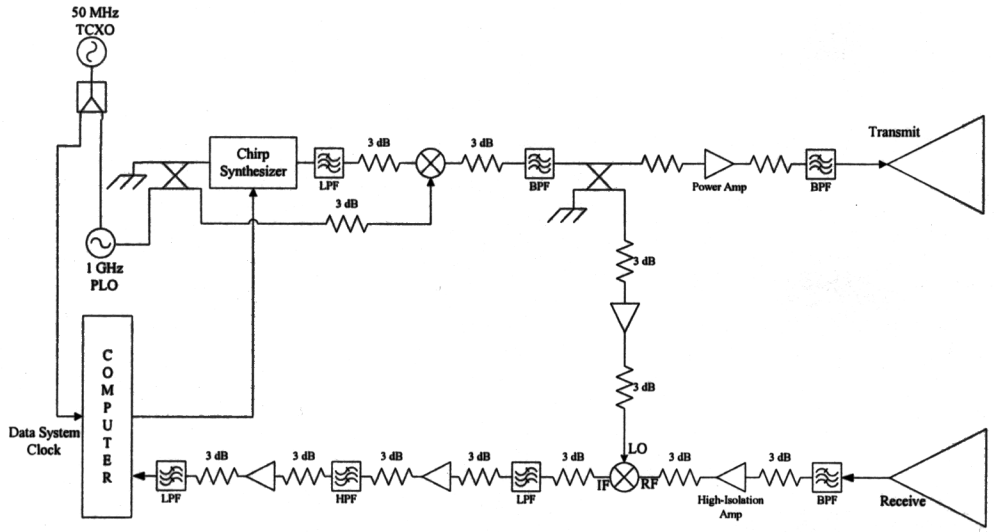

Figure 1. Block diagram of the 600-900 MHz FM-CW radar for high-resolution layer mapping.

The wideband radar data must be converted into a range profile to generate high-resolution radar echograms. A range profile is obtained by generating the frequency spectrum of the beat signal with a Fourier transform algorithm. Prior to the transformation, we multiply the data with a suitable window function such as Hamming, Hanning or Blackmann to reduce sidelobe levels. Next, the data are passed through a "dewow" filter to remove any DC bias and bring out the higher frequency events. To increase the signal-to-noise ratio a number of traces—based on airspeed and surface topography—are averaged coherently. Finally, the data are multiplied by a function that increases the gain as a function of depth for amplifying deeper reflections that experience large attenuation due to spherical spreading and absorption and scattering.

2.2.1 High-resolution wideband radar results

Figure 2a shows the comparison between measurements made with our system over the NASA-U1 site (73.84°N, 49.49°W) and the ice core record. The reflection coefficient was computed from the density contrast obtained from on-site ice core data. The reflections from our measurements have been successfully matched to the ice core record to within ± 1 m.

Figure 2b shows the result of internal layers observed with our radar system over a 147-km traverse in the dry-snow zone of North Greenland. The wave velocity in firn has not been corrected in this figure. The figure shows a multitude of internal layers up to a depth of about 250 m, with many layers tracked across the entire flight path.

Figure 2c shows the layers that were observed while transitioning from the percolation zone to the wet-snow zone. This zone is characterized by surfaces with wet or saturated snow at a temperature of 0° C. The depths are plotted relative to aircraft height. As expected, only a few layers can be observed since wave penetration is severely limited by the presence of wetness on the surface. We are able to observe reflections up to a depth of about 20 m below the surface, which can provide accumulation history over more than 20 years. We can also note how the separation between the layers increases as we move from the lower accumulation zone to the higher accumulation zone.

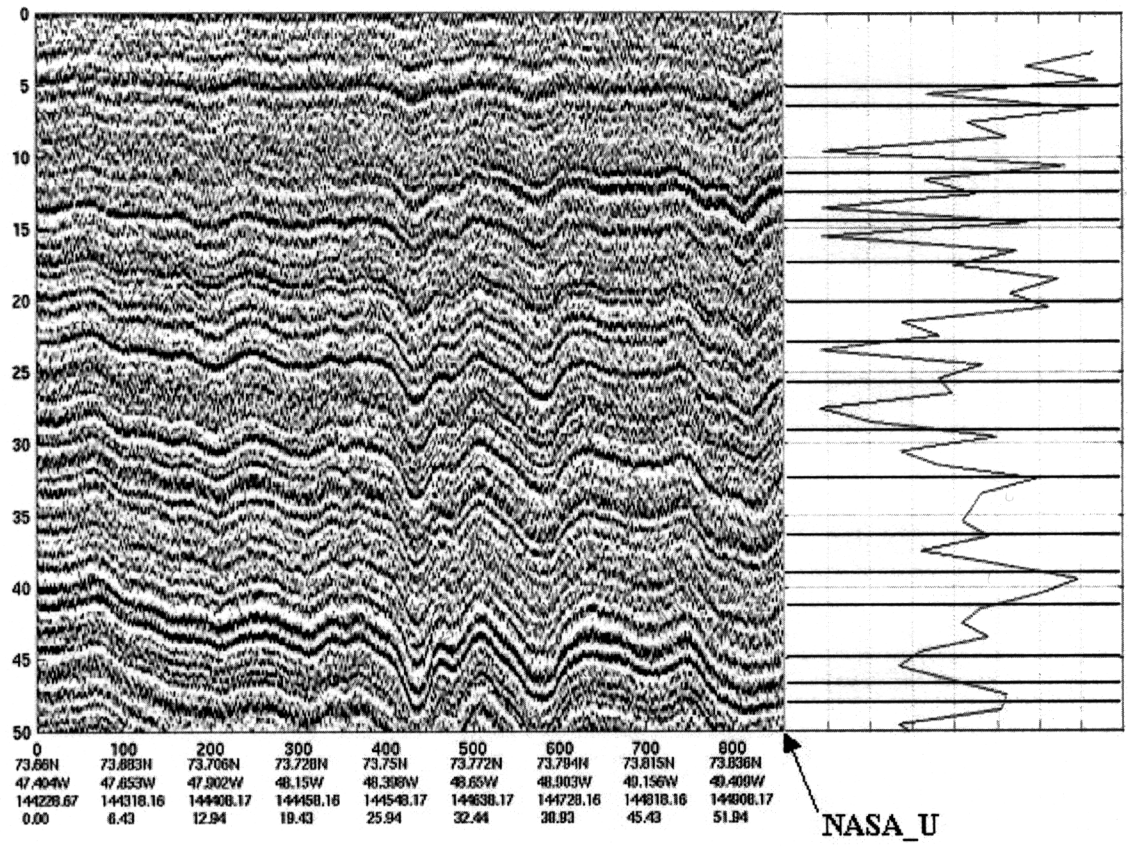

Figure 2a. Comparison between airborne radar measurements and ice core records.

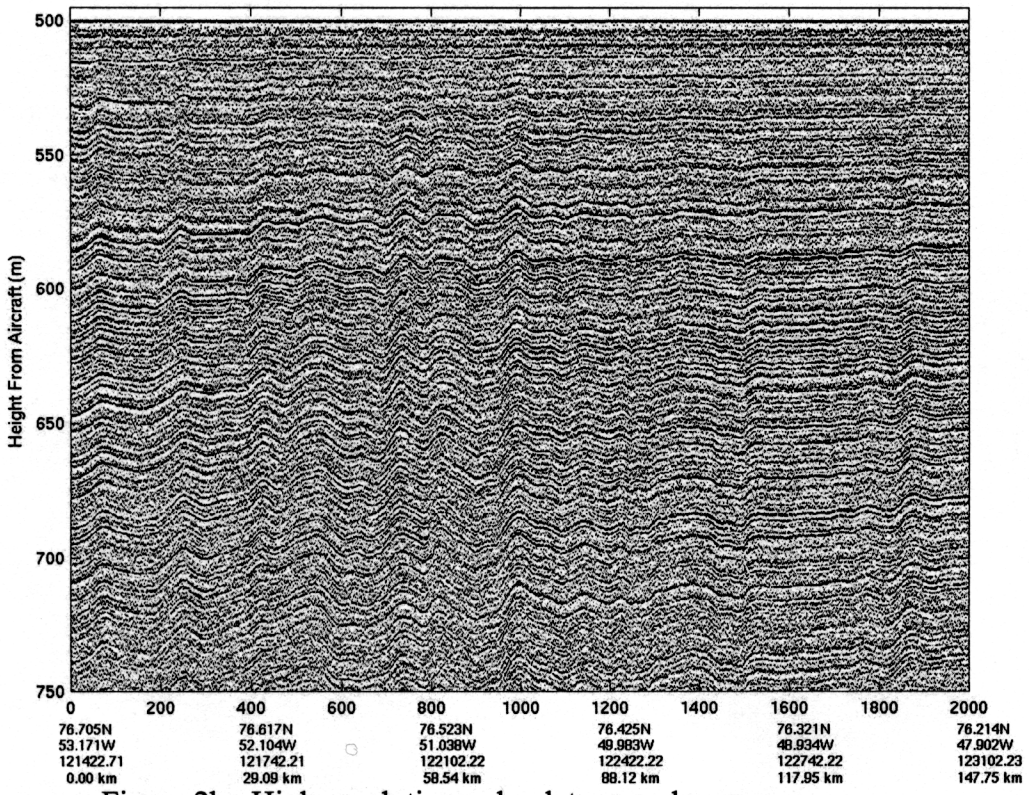

Figure 2b: High-resolution radar data over dry snow zone.

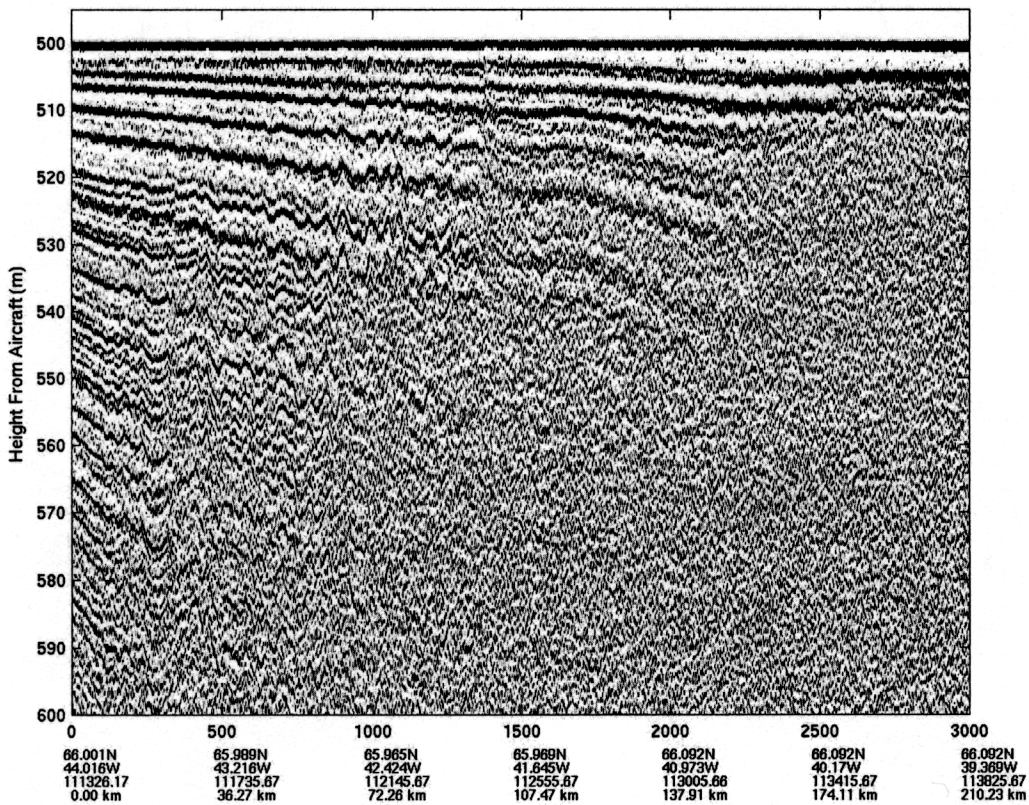

Figure 2c. Transition from percolation to wet-snow zone.

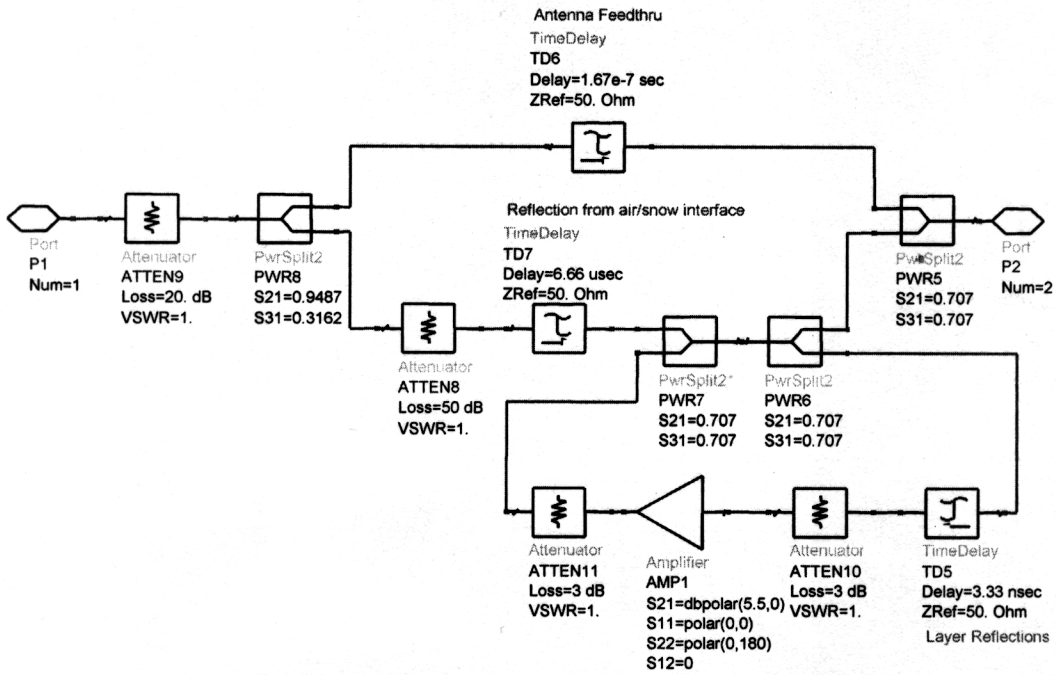

Figure 3. Block diagram of the target for simulating surface and subsurface returns.

2.3 Development of a calibrator for the wideband radar

For optimizing radar performance, we developed a radar target simulator using optical and microwave delay lines for simulating reflections from the glacial ice surface and internal layers spaced about every 50 cm with appropriate amplitude distribution. The simulator was developed to conduct laboratory tests to optimize the radar performance and signal processing algorithms, and to calibrate the radar in the field.

Figure 3 shows the block diagram of the simulator. The transmitter signal is applied to the input port of the simulator, labeled port-1. The input signal is passed through an attenuator (ATTEN9) and supplied to the input port of a power divider (PWR8) for splitting the signal into two parts. One part is passed through the RF delay line (TD6) to one of the input ports of the output power combiner (PWR5) at port-2. This signal simulates the feedthrough signal between the antennas. The other output signal from the input power divider (PWR8) is passed through a 50-dB attenuator (ATTEN 8) to an RF/Optical transceiver (not shown in figure) in which the long-chirped transmitter signal at 600-900 MHz is converted into an optical frequency.

This optical signal is passed through a 500-m-long optical fiber (TD7) to simulate transit delay associated with propagation from the radar antennas to the firn surface and back. The optical fiber output is converted back into the 600-900 MHz range using an Optical/RF transceiver (not shown in figure). The RF output from the transceiver is passed through a power combiner (PWR7) and a power divider (PWR8) to one of the input ports of the output power combiner (PWR5). The output from the second port of the power divider (PWR8) is passed through a transmission line (TD5) to simulate delay associated with propagation from the firn surface to an internal layer. The delay output is passed through a 3-dB attenuator (ATTEN 10), an amplifier (AMP1) and another 3-dB attenuator (ATTEN 11) to the second input port of the power combiner (PWR7). The attenuators are used to buffer the amplifier

and reduce multiple reflections. The gain of the feedback loop—comprising the power combiner (PWR7), power divider (PWR8), the transmission line, and the buffered amplifier—is selected to less than one. This loop simulates returns from many internal layers with spacing between layers of about 50 cm. The output signal from the simulator available at port-2 is injected into the receiver for calibration.

2.4 Standardizing signal processing procedures

We have standardized the signal processing techniques applied to the radar depth sounder data. The routine signal processing procedures now include:

DC Removal: DC signal components are removed from the radar signal by calculating the mean of the noise present and subtracting this from both the Inphase (I) and Quadrature (Q) signals.

Gain Compensation: This procedure normalizes a data series segment (echogram) to compensate for gain setting changes made by the radar operator during data collection.

Coherent Noise Reduction: The I and Q radar signals have both a coherent, non-random component and a non-coherent, random component. The non-random signal component is caused by antenna reflections, reflections in the RF section of the radar, and leakage signals. The random signal component results from scattering throughout the ice column. An estimate of the coherent term can be computed by coherently averaging over a set of spatially distributed measurement samples. The coherent noise component may then be removed from the signal by subtracting this coherently averaged value from each individual measurement. All that remains after the **Coherent Noise Reduction technique** has been applied is the non-coherent term, and the noise present is only white noise.

Filtering: After coherent noise reduction, the signal is then passed through a windowing function, which aims to replace the radar receiver transfer function with a uniform Hamming window transfer function to further reduce the sidelobes and noise level. This results in a 2- to 3-dB improvement in the signal.

Multiple Removal: This process removes the first multiple echo from the surface using the principle that the first multiple echo and the zero return are equidistant from the surface echo.

Coherent and Incoherent Integrations: This process puts the signal in a form for viewing which requires the data to be highly averaged. The coherent integrations are performed on the I and Q linear data and the incoherent integrations are performed on the non-linear amplitudes (A, the scalar magnitude of the I and Q data). The number of coherent and incoherent integrations is chosen accordingly to allow each record in the along track direction to be one second apart.

Inter Gain Compensation: This process compensates for gain setting changes across adjacent signal data files.

Compensation of signal attenuation: The EM wave is attenuated by approximately 20 to 25 dB per kilometer of ice. To compensate for this attenuation, an exponential gain is applied to the signal, varying from 0 dB at the ice surface to 20 dB at the last range bin.

3.0 Publications, presentations, and reports associated with this project: 1999 - 2001

3.1 KU Investigators

3.11 Refereed Papers

Kanagaratnam, P., S. P. Gogineni, N. Gundestrup & L. Larsen, "High-resolution radar mapping of internal layers at NGRIP," *J. Geophysical Research (Climate & Physics of the Atmosphere)* special issue on Program for Arctic Regional Climate Assessment (PARCA), 2001.

Gogineni, S., D. Tammana, D. Braaten, C. Leuschen, T. Akins, J. Legarsky, P. Kanagaratnam, J. Stiles, C. Allen & K. Jezek, "Coherent radar ice thickness measurements over the Greenland ice sheet," *J. Geophysical Research (Climate & Physics of the Atmosphere)* special issue on PARCA, 2001.

Legarsky, J. J., P. Gogineni & T. L. Akins, "Focused synthetic-aperture radar processing of ice-sounder data collected over the Greenland ice sheet," *IEEE Trans. on Geoscience and Remote Sensing,* vol. 39, no. 10, pp. 2109-2117, 2001.

Braaten, D., S. Gogineni, D. Tammana, S.K. Namburi, J. Paden, and K. Gurumoorthy, "Improvement of radar ice thickness measurements of Greenland outlet glaciers using SAR processing," in press, *Annals of Glaciology*, 2001.

3.12 Conference Presentations

Kanagaratnam, P., S. Gogineni, J. Legarsky, T. Akins, N. Gundestrup, L. Larsen & J. Kipfstuhl, "High-Resolution Monitoring of Internal Layers at NGRIP," *IGARSS'99 Digest*, 28 June to 2 July, Hamburg, Germany, pp. 95-97, 1999.

Legarsky, J. J., S. P. Gogineni, P. Kanagaratnam, T. L. Akins & Y. C. Wong, "Ice Thickness Measurements of the Southwest Greenland 2000-m Contour Line," *IGARSS'99 Digest*, 28 June to 2 July, Hamburg, Germany, pp. 89-91, 1999.

Gogineni, S. & P. Kanagaratnam, "Wideband Radar for Determination of Snow Accumulation over the Greenland Ice Sheet," *Proceedings of the 26th General Assembly of URSI,* 13-21 August, Toronto, Canada, p. 722, (invited presentation),1999.

Gogineni, S. & P. Kanagaratnam, "Wideband radar for Determination of Snow Accumulation over the Greenland Ice Sheet," presented at the Eighth Int. Conference on Ground Penetrating Radar (GPR'2000), 23-26 May, Gold Coast, Australia, 2000.

Kanagaratnam, P., Gogineni, S., N. Gundestrup & L. Larsen, "High-Resolution Monitoring of Internal Layers over the Greenland Ice Sheet," *IGARSS'2000 Digest*, 00CH37120, Honolulu, 24-28 July, pp. 460-462, 2000.

Leuschen, C., S. Gogineni & D. Tammana, "SAR Processing of Radar Echo Sounder Data," *IGARSS'2000 Digest*, 00CH37120, Honolulu, 24-28 July, pp. 2570-2572, 2000.

Kanagaratnam, P., R. Eakin & S. Gogineni, "An Airborne Radar System for High-Resolution

Mapping of Internal Layers," presented at IGARSS'01, 9-13 July, Sydney, Australia, 2001.

P. Kanagaratnam, B. Parthasarathy, T. Plummer, T. Akins, D. Braaten and S.P. Gogineni, "A High-Resolution Airborne Radar System for Near Surface Mapping of Internal Layers to Estimate Accumulation Rate," Proceedings, 32nd European Microwave Conference, September, 24 – 26, 2002, Milan, Italy.

Braaten, D.A. and S. Gogineni, "Radar measurements of ice sheet thickness of outlet glaciers in Greenland," Proceedings, International Geoscience and Remote Sensing Symposium (IGARSS), Toronto, 2002.

3.13 KU Technical Reports

Legarsky, J. "SAR Processing of Glacial-Ice Depth-Sounding Data, Ka-Band Backscattering Measurements and Applications," Radar Systems and Remote Sensing Laboratory Technical Report 13720-8, 1999.

Tee, K. L., W. K. Chong, H. Coulter, T. Akins, S. P. Gogineni, C. Allen & J. Stiles, "Radar Thickness Measurement over the Southern Part of the Greenland Ice Sheet: 1998 Results," Radar Systems and Remote Sensing Laboratory Technical Report 13720-10, July 1999.

Gogineni, S. P., C. Allen & J. Stiles, "Measurement of thickness of the Greenland ice sheet and investigation of scattering properties of glacial ice: Final report," Radar Systems and Remote Sensing Laboratory Technical Report 13720-11, October 2000.

3.14 KU Theses and Dissertations

Legarsky, J., "Synthetic-aperture radar (SAR) processing of glacial-ice depth-sounding data, Ka-band backscattering measurements and applications," Ph.D. dissertation, University of Kansas, 1999.

Akins, T., "Design and development of an improved data acquisition system for the coherent radar depth sounder," M.S. thesis, University of Kansas, 1999.

Tammana, D., "Design of waveform generator for coherent radar depth sounder," M.S. thesis, University of Kansas, 2001.

Eakin, R., "Design and development of a one gigasample per second radar data acquisition system," M.S. thesis, University of Kansas, 2001.

Kanagaratnam, P., "Airborne radar for high resolution mapping of internal layers in glacial ice to estimate accumulation rate," Ph.D. dissertation, University of Kansas, 2002.

3.2 Work by Other Scientists and Investigators with KU Participation

3.21 Refereed Papers

Joughin, I., M. Fahnestock, R. Kwok, P. Gogineni & C. Allen, "Ice flow of Humboldt, Petermann, and Ryder Glaciers," *J. Glaciology*, vol. 45, no. 150, pp. 231-241, 1999.

Forster, R. R., K. C. Jezek, J. Bolzan, F. Baumgartner & S. P. Gogineni, "Relationships between radar backscatter and accumulation rates on the Greenland ice sheet," *Int. J. Remote Sensing,* vol. 20, nos. 15 & 16, pp. 3131-3147, 1999.

Thomas, R., T. Akins, B. Scatho, M. Fahnestock, P. Gogineni, C. Kim & J. Sonntag, "Mass balance of the Greenland ice sheet," *Science*, vol. 289, no. 5478, pp. 426-428, 21 July 2000.

Rignot, E., G. Buscarlet, B. Csatho, S. Gogineni, W. Krabill & M. Schemetz, "Mass balance of the northeast sector of the Greenland ice sheet: A remote sensing perspective," *J. Glaciology,* vol. 46, pp. 265-273, 2000.

Thomas, R. H., W. Abdalati, T. L. Akins, B. M. Csatho, E. B. Frederick, S. P. Gogineni, W. B. Krabill, S. S. Manizade & E. J. Rignot, "Substantial thinning of a major east Greenland outlet glacier," *Geophysical Research Letters*, vol. 27, no. 9, pp. 1291-1294, May 2000.

Baumgartner, F., J. Munk, K. C. Jezek & P. Gogineni, "On reconciling surface-based with surface backscatter measurements," submitted to *Int. J. Remote Sensing*, 2001.

Thomas, R. H., S. P. Gogineni & other PARCA investigators, "Program for arctic regional climate assessment (PARCA): Goals, key findings, and future directions," *J. Geophysical Research (Climate & Physics of the Atmosphere)* special issue on PARCA, 2001.

Bamber, J. L., R. L. Layberry & S. P. Gogineni, "A new ice thickness and bedrock data set for the Greenland ice sheet: Part I," *J. Geophysical Research (Climate & Physics of the Atmosphere)* special issue on PARCA, 2001.

Fahnestock, M. A., I. Joughin, T. A. Scambos, R. Kwok, W. B. Krabill & S. Gogineni, "Ice-stream related patterns of ice flow in the interior of northeast Greenland," *J. Geophysical Research (Climate & Physics of the Atmosphere)* special issue on PARCA, 2001.

Fahnestock, M., W. Abdalati, S. Luo & S. Gogineni, "Internal layer tracing and age-depth-accumulation relationships for the northern Greenland ice sheet," *J. Geophysical Research (Climate & Physics of the Atmosphere)* special issue on PARCA, 2001.

Rignot, E., S. P. Gogineni, I. Joughin & W. B. Krabill, "Contribution to the glaciology of northern Greenland from satellite radar interferometry," *J. Geophysical Research (Climate & Physics of the Atmosphere)* special issue on PARCA, 2001.

3.2.2 Conference Presentations

Baumgartner, F., K. Jezek, R. R. Forster, S. P. Gogineni & I. H. H. Zabel, "Spectral and Angular Ground-Based Radar Backscatter Measurements of Greenland Snow Facies," *IGARSS'99 Digest*, 28 June to 2 July, Hamburg, Germany, pp.1053-1055, 1999.

Munk, J., K. Jezek, F. Baumgartner, S. P. Gogineni, R. Forster & I. H. H. Zabel, "Estimating a Volumetric Backscatter Coefficient from In-Situ Measurements in the Greenland Ice Sheet," *IGARSS'2000 Digest*, 00CH37120, Honolulu, 24-28 July, pp. 917-919, 2000.

Layberry, R. L., J. L. Bamber & S. P. Gogineni, "A New Ice Thickness and Bedrock Data Set for the Greenland Ice Sheet," *IGARSS'2000 Digest*, 00CH37120, Honolulu, 24-28 July, pp. 1134-1136, 2000.